Understanding the Role of Intra- and Intermolecular Interactions in the Formation of Single- and Double-Helical Structures of Aromatic Oligoamides: A Computational Study

Hao Dong, Shugui Hua, and Shuhua Li*

Institute of Theoretical and Computational Chemistry, Key Laboratory of Mesoscopic Chemistry of Ministry of Education, School of Chemistry and Chemical Engineering, Nanjing University, Nanjing, 210093, P. R. China

Received: August 11, 2008; Revised Manuscript Received: December 18, 2008

The generalized energy-based fragmentation (GEBF) approach has been implemented to extend the applications of density function theory (DFT) with empirical van der Waals (vdW) correction (Wu, Q.; Yang, W. T. *J. Chem. Phys.* 2002, *116*, 515.) to large supramolecular systems with extensive $\pi-\pi$ stacking interactions. This mixed approach, DFT(vdW)-GEBF, is applied to investigate the energies and structures of several aromatic oligoamide foldamers. Our calculations show that the formation of single helical structures is mainly driven by the stacking interaction between neighboring aromatic rings, further stabilized by the intramolecular hydrogen bonds of the backbone. The dimerization of two single helical strands to form the double helical structure is an energetically favorable process, which is mainly driven by extensive interstrand aromatic−aromatic interactions. However, the dimerization energy tends to decrease significantly for longer oligomeric strands.

1. Introduction

Artificial oligomers that can fold or assemble into well-defined conformations have received considerable interests in recent years.[1−13] It has been recognized that the folding or assembling processes are controlled by inter- and intramolecular noncovalent interactions, including hydrogen bonding, aromatic stacking, and so on.

For example, aromatic oligoamides based on 2,6-diaminopyridine and 2,6-pyridine dicarboxylic acids (AOA's)[14−21] were found to fold into very robust single helical conformers, which further assemble to form double helical dimers. The crystal structures obtained in the solid state and NMR spectroscopic studies in solution suggested that intramolecular hydrogen bonds (H-bonds) and aromatic stacking interactions might induce bending of molecular strands into single helices, and interstrand aromatic−aromatic interactions might be the primary driving force for the formation of double helical dimers. It should be emphasized that the double helices formed by the dimerization of the pyridine carboxamide oligomers are very different from natural double helices (like DNA or Gramicidine D[22]) that are mainly based on interstrand hydrogen bonding.[23,24] Experiments showed that the dimerization of single helices of AOA's to form double helices increases with strand length to reach a maximum and then decreases down to undetectable levels for longer oligomers.[25] Although some computational studies based on force field methods have been performed to understand some of the thermodynamic and kinetic factors in the folding or assembling processes for AOA's,[26] further theoretical studies based on more accurate quantum mechanical calculations are still desirable. Especially, the following two issues have not been well understood: (1) the relative contributions of intramolecular H-bonds and aromatic stacking into the formation of single helical conformers; (2) the interstrand interaction energies for two single helices to form double helices and their dependence on the strand length.

On the other hand, accurate quantum mechanical calculations on the van der Waals (vdW) interactions have been limited to small molecules, because the accurate descriptions of the vdW energy require computationally demanding post-Hartree−Fock (post-HF) methods (such as second-order Møller−Plesset, MP2) and very large basis sets.[24,27−30] In recent years, many groups have investigated the stacking interactions between base pairs, or between aromatic rings, with these post-HF methods.[31−46] It is generally accepted that the stacking interactions are mainly determined by the dispersion energy.[30] However, it is computationally prohibitive for these post-HF methods to extend to large systems involved in supramolecular chemistry. Fortunately, it has been shown that the density function theory (DFT) with popular exchange-correlation functionals, corrected by an empirical vdW term (which can be easily calculated), could provide a promising alternative to the computationally expensive post-HF methods.[47−58] Test applications have demonstrated that density functional calculations with vdW corrections could provide quantitatively good results on the aromatic stacking interactions comparable to MP2 calculations. Nevertheless, even for DFT calculations, we also need linear scaling algorithms to extend their applications to systems with hundreds of atoms.[59−82] In our previous work, we have developed a generalized energy-based fragmentation approach (GEBF)[83−85] for performing approximate quantum mechanical calculations, which are applicable within various theoretical frameworks (HF, DFT, post-HF) for very large systems. The main idea of this method and similar other methods[77,78] is to calculate the total energy of a large molecule from energy calculations on a series of small subsystems. This simple approach was found to give quite satisfactory results for ground-state energies and optimized geometries for neutral or charged closed-shell systems.[83−85]

In this work, we will apply the GEBF approach within the vdW-corrected DFT framework to investigate the energetics of the folding and assembling processes for several AOA's, which have been characterized experimentally. We will try to address the two problems described above for studied systems. The results from this study will provide some insight into the role of the intra- and intermolecular interactions in controlling the formation of single and double helical structures.

* Corresponding author. E-mail: shuhua@nju.edu.cn.

10.1021/jp8071525 CCC: $40.75
Published on Web 01/26/2009

2. Computational Details

The details of the GEBF approach have been described in our previous work.[83−85] Here we only give a brief introduction on the basic idea of this approach. The main procedures include: (1) divide the whole system into fragments of comparable size; (2) construct subsystems for all fragments, according to some defined rules; (3) put each subsystem in the presence of background point charges (which are used to model distant fragments outside the given subsystem); (4) perform conventional quantum chemistry calculations for all "electronically embedded" subsystems; (5) obtain the total energy of the target molecule according to eq 1

$$E_{tot} = \sum_{m}^{M} C_m \tilde{E}_m - (\sum_{m}^{M} C_m - 1) \sum_{A} \sum_{B>A} \frac{Q_A Q_B}{R_{AB}} \qquad (1)$$

where E_{tot} is the total energy of the target system, $\tilde{E}_m$ is the energy of the mth subsystem including the self-energy of point charges, C_m is the coefficient of the mth subsystem, and Q_A is the point charge on atom A.

In the vdW-corrected DFT method, an additional vdW attraction energy term is added to the total energy calculated from standard density functional calculations. Thus, the total energy, with vdW correction, has the following form

$$E_{tot}^{corr} = E_{tot} + E_{vdw} \qquad (2)$$

In this work, the vdW term derived from Wu and Yang[47] is adopted. The total vdW energy is calculated as the sum of the contributions from all the atom pairs,

$$E_{vdW} = \sum_{i=1}^{all-1} \sum_{j=i+1}^{all} E_{ij,vdw} = -\sum_{i=1}^{all-1} \sum_{j=i+1}^{all} f_d(R) \frac{2(C_{6ii}^{\ 2} C_{6jj}^{\ 2} N_i N_j)^{1/3}}{(C_{6ii} N_j^{\ 2})^{1/3} + (C_{6jj} N_i^{\ 2})^{1/3}} \frac{1}{R_{ij}^{\ 6}} \qquad (3)$$

$$f_d(R) = \left[1 - \exp\left(-\frac{kR_{ij}^{\ 3}}{R_m^{\ 3}}\right)\right]^2 \qquad (4)$$

Here $f_d(R)$ is a damping function which equals to 1 at large value of R and 0 at small value of R, k is the damping coefficient with the value of 3.54, R_{ij} is the distance between atoms i and j, and R_m is the sum of the atomic vdW radii for atoms i and j. In addition, C_{6ii} is the atomic C_6 coefficient for atom i−atom i pair, and N_i is the effective number of electrons for atom i. These parameters are all from the original paper of Wu and Yang.[47] It should be mentioned that only parameters for H, C, N, and O atoms are available, and for C and O atoms, different atom type are used to account for the corresponding bonding environments. Since the combination of Becke's three parameter hybrid functional with the Lee−Yang−Parr correlation functional (B3LYP) with the vdW correction was demonstrated to provide the overall good performance, we will employ only B3LYP functional for DFT calculations in this paper. The vdW-corrected B3LYP calculations will be abbreviated as B3LYP(vdW) for simplicity.

To conclude from discussions above, we will calculate the total molecular energy of a large molecule by summing up the total B3LYP energy from the GEBF approach and the total vdW energy. This mixed approach is called as B3LYP(vdW)-GEBF hereafter. Since the analytical gradients of the total DFT energy can be approximately obtained from corresponding calculations on small subsystems within the GEBF approach,[83−85] and the gradients of the total vdW energy are easily computed, the B3LYP(vdW)-GEBF approach can easily be applied for geometry optimizations of large molecules.

To investigate the weakly bonded complexes with the GEBF approach, an important issue to be addressed is how to calculate the basis set superposition error (BSSE) with counterpoise (CP) correction.[86] Take a double helical structure as an example. With the GEBF approach, one can easily compute the energies of two single strands and the corresponding double-helical dimer. In addition, one also needs to calculate the energies of two single strands, with atoms in another strand as ghost atoms (basis functions on ghost atoms are available for calculation on a single strand). With the GEBF approach, one may calculate the energy of a single strand (with ghost atoms in another strand) with the following procedure. First, a series of subsystems are constructed for this single strand as if another strand does not exist. Then, for a given subsystem, some ghost atoms in another strand, which are spatially close to any atoms in this subsystem, are included in calculation on this subsystem. A distance threshold (4 Å) is set to pick up neighboring ghost atoms. Those basis functions beyond this distance threshold in another strand usually make negligible contributions to the energy of this subsystem, and can be neglected without much loss of accuracy. Test calculations show that the BSSE calculated with the GEBF approach is very close to that obtained from conventional full system calculations (one example is given in the next subsection). On the other hand, a recent review[44] pointed out that 50% but not the full BSSE correction often yields more reasonable results on the binding energies between weakly bonded components, especially in treating weakly bonded complexes consisting of two large molecules. So 50% BSSE correction is employed in computing the binding energies in this work.

All the conventional DFT calculations for the studied systems and their subsystems are performed with the Gaussian 03 program.[87] The B3LYP(vdW)-GEBF approach has been implemented in the LSQC package developed in our group.[83−85]

3. Results and Discussions

In this subsection, we will employ the B3LYP(vdW)-GEBF approach to investigate the energies and optimized structures of two single-helical molecular strands (**A**[16] and **B**[18]) and two double-helical foldamers (**C**[88] and **D**[89]) based on aromatic oligoamides (Figure 1). The repeating units in these oligomers differ from each other by substituents in position 4 of the pyridine rings. First, for the single helical strand **A**, we will calibrate the accuracy of the B3LYP(vdW)-GEBF approach by comparing the energies and structures obtained from this approach with those from the conventional B3LYP(vdW) calculations. Then, the B3LYP(vdW)-GEBF approach will be used to study the role of intra- and intermolecular interactions in the formation of single helices (**A** and **B**), and double helices (**C** and **D**).

Before doing GEBF calculations, it is necessary to divide the studied systems into fragments of comparable size. The fragmentation schemes for these systems are provided in the Supporting Information (Figure S1). Also, the only parameter, the maximum number of fragments for subsystems (η), should be set for a GEBF calculation. Usually, a large value of η gives more accurate energies, but an optimal value exists for η, beyond which the accuracy of the approach cannot be further improved. After doing test calculations, we find that $\eta = 5$ is appropriate for systems under study. With this parameter, the largest subsystem in our GEBF calculations will only have about 50−60 atoms, which can be efficiently calculated with standard DFT methods implemented in the Gaussian 03 package.

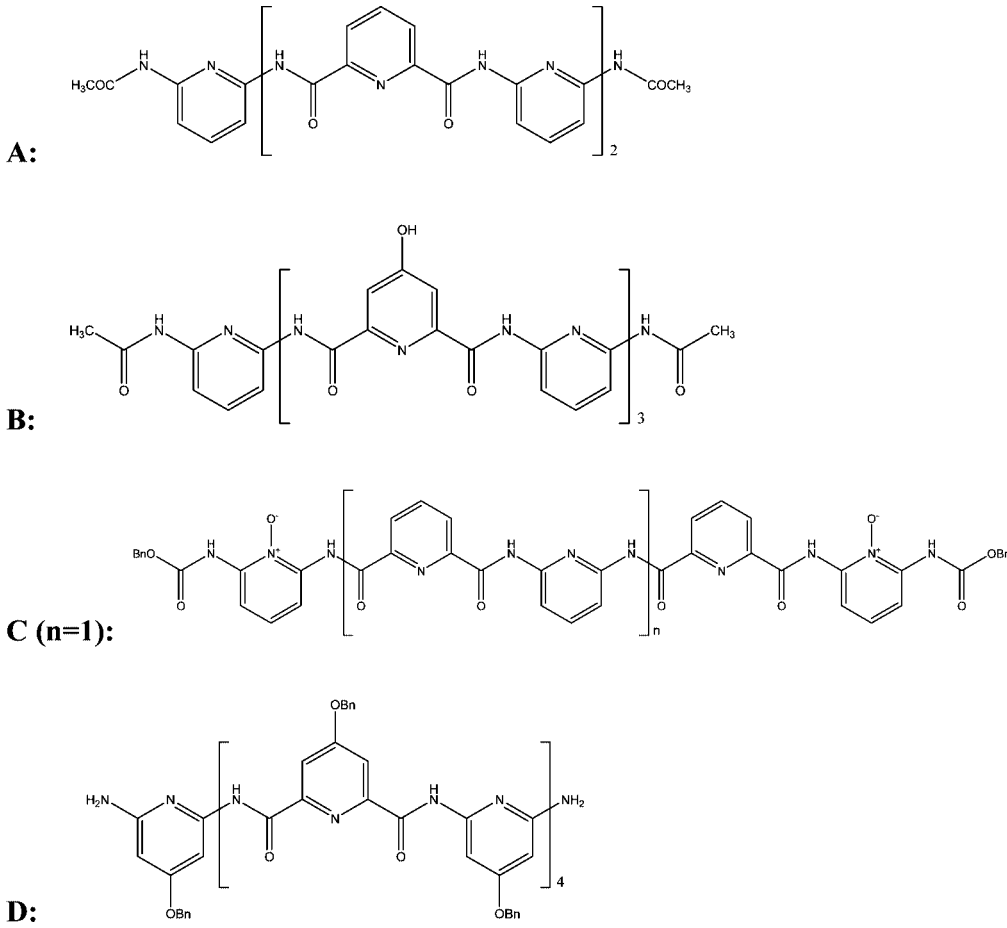

Figure 1. Structures of oligomers **A**−**D**.

TABLE 1: Optimized Structures (Distance is in Å) Obtained by Different Methods with the 6-31G Basis Set for Oligomer A. The interlayer distances (d_1−d_4) are shown in Figure 2**

method		d_1 (N−N)	d_2 (N−N)	d_3 (N−N)	d_4 (O−O)	rmsd
crystal structure[a]		3.549	3.473	3.731	7.111	0.00
B3LYP		4.032	3.838	4.032	7.163	0.41
B3LYP(vdW)		3.328	3.303	3.436	7.215	0.38
B3LYP(vdW)-GEBF	charge	3.326	3.299	3.434	7.212	0.38
	no charge	3.326	3.300	3.433	7.213	0.38

[a] The data is from ref 16.

In order to compare the optimized structure with the experimental crystal structure, we will use the root-mean-square deviation (rmsd) between the two structures as a measurement. The analysis is done with VMD program.[90]

3.1. Calibration of the B3LYP(vdW)-GEBF Approach. For oligomer **A**, its crystal structure[16] can be used to calibrate the optimized geometries obtained from the conventional B3LYP approach (with and without vdW corrections) and the B3LYP-GEBF approach (Table 1). As show in Table 1, the geometry obtained from conventional B3LYP/6-31G** calculations is quite different from the crystal structure.[16] The calculated interlayer distance is about 0.3∼0.5 Å longer than the corresponding value in the crystal structure. However, we find that the structure optimized from B3LYP(vdW)/6-31G** calculations is much closer to the crystal structure. The B3LYP(vdW)-GEBF approach leads to a optimized structure almost identical to that given by the conventional B3LYP(vdW) calculation. In addition, the difference between B3LYP(vdW) and B3LYP(vdW)-GEBF energies calculated at the optimized B3LYP(vdW)-GEBF/6-31G** geometry is only 1.56 kcal/mol. Thus, the GEBF approach is expected to give quite accurate energies and optimized geometries for all systems under study. On the other hand, the difference between B3LYP and B3LYP(vdW) geometries demonstrates that the dispersion energy is vital for describing the stacking interaction between aromatic rings and the B3LYP method without the vdW correction is not capable of giving accurate predictions for molecules with overlapping aromatic rings such as **A**. This point was also demonstrated by a recent work, which shows that the loss of dispersion energy could result in the transformation of DNA from double-helix to ladder-like structure.[91] It should be mentioned that in the crystal structure of **A** two hydrogen bonds between the solvent methanol and the terminal acetamide group can be found. This interaction, which may increase the interlayer distance in **A**, is not taken into account in all calculations described above. The neglect of two hydrogen bonds in our calculations may provide an explanation on why the d3 distance (about 3.4 Å) calculated with conventional B3LYP(vdW) or B3LYP(vdW)-GEBF calculations is significantly shorter than the value in the crystal structure (3.7 Å). In addition, we do not consider the crystal field effects in our calculations. Since the purpose of this work is to investigate the intrinsic driving forces for oligomers **A**−**D**

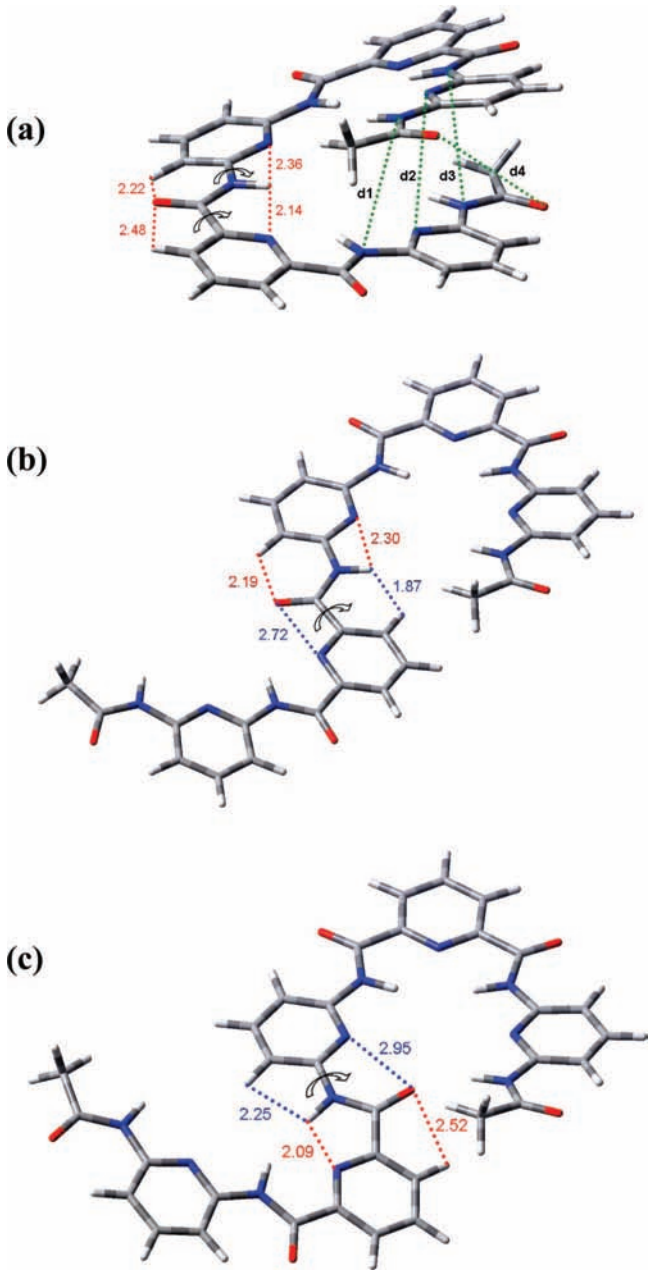

Figure 2. Optimized structures of oligomer **A**: (a) helical structure; (b) extended-1 structure (by rotating the CO−aryl bond); (c) extended-2 structure (by rotating the NH−aryl bond).

to form specific single-helical or double-helical structures, the neglect of hydrogen bonds (between these molecules and their nearby solvents) and crystal field effects will not change the qualitative picture obtained from this study.

For the B3LYP(vdW)-GEBF approach, we also investigate the influence of background point charges on the optimized structure (Table 1). For the 6-31G** basis set, we notice that the optimized structure without point charges ($Q_A = 0$ for all atoms in eq 1) is almost the same as the optimized structure with background point charges. This result suggests that the electrostatic and polarization interactions between remote fragments in **A** contribute little to the total energy. Since the other systems under study are structurally similar to **A**, we will not include background point charges in the B3LYP(vdW)-GEBF calculations for all systems **A**−**D**.

To achieve a compromise between accuracy and computational cost, the B3LYP(vdW)-GEBF approach with the 6-31G** basis set will be used to optimize the structures of all oligomers **A**−**D** in the following subsection. Then, the same approach with a larger basis set 6-311+G** will be used to perform single point calculations to get more accurate energies. Solvent molecules will be excluded in calculations for simplicity.

3.2. The Intramolecular Interaction for the Formation of Single Helical Structures for Oligomers A and B. As revealed from the crystal structures, oligomers **A** and **B** exhibit well-defined single-helical structures with one turn (**A**), and one and a half-turn (**B**), respectively. B3LYP(vdW)-GEBF/6-31G** calculations can reproduce the crystal structures of compounds **A** and **B** with good accuracy. As shown in Table 2, the rmsd between the crystal structure and the optimized structure is less than 0.4 for both single-helical structures **A** and **B**. Thus, the B3LYP(vdW)-GEBF approach performs quite well in predicting the geometries of these two foldamers. The calculated mean helical pitch (Table 3) is 3.47 Å for **A**, 3.36 Å for **B**. This result suggests that the helical structure becomes more contracted with increasing the oligomer length. This effect may be ascribed to the additional stabilization interaction from the cooperative $\pi-\pi$ interactions between neighboring layers. Our results are in accord with the experimental facts that the stability of single helices is enhanced in longer oligomers.[25]

To understand the driving forces for the formation of the single helical structures for **A** and **B**, we will perform some additional calculations for compound **A**. Our aim is to investigate: (1) whether the helical structure of **A** is the lowest-energy conformer among various possible conformers? (2) During the formation of the helical structure from extended structures, how large is the contribution from the $\pi-\pi$ interaction between neighboring aromatic rings?

To address the two questions described above, we need to construct some extended structures for oligomer **A**. Obviously, one can obtain many extended structures by rotating the CO−aryl bond (between the carbonyl group and the pyridine group), or the NH−aryl bond (between the NH group and the pyridine group).[92] For example, by rotating one of the CO−aryl bonds or one of the NH−aryl bonds in the helical structure, one can generate two extended structures (denoted as extended-1 or extended-2), as shown in Figure 2. These extended structures are then freely optimized with the B3LYP(vdW)-GEBF approach with the 6-31G** basis set. The total energies of these two structures and the helical structure are listed in Table 4 for comparison.

It can be seen that both extended structures are significantly higher in energy than the helical structure. For instance, the extended-2 structure is 14.1 kcal/mol above the helical structure. It may be worthwhile to give a qualitative analysis for this result. First, one can see (from Figure 2) that there are many intramolecular hydrogen bonds (for instance, C═O···H−C(pyridine) and N−H···N(pyridine)) along the backbone of the helical structure, due to the trans arrangement between the NH group and its neighboring carbonyl group. In contrast, in the extended-2 structure, the rotation of one NH−aryl bond breaks two attractive hydrogen bonds (C═O···H−C(pyridine) and N−H···N(pyridine)), and the attractive $\pi-\pi$ interaction between partially overlapping pyridine rings. Furthermore, two interactions, C═O···N(pyridine) ($R_{O...N}$=2.95 Å) and N−H···H−C(pyridine) ($R_{H...H} = 2.25$ Å), are introduced in the extended-2 structure (as shown in Figure 2). These two interactions are repulsive, because, for example, the O···N distance in the C═O···N(pyridine) contact is shorter than the sum of the vdW radius of these two atoms (1.55 Å for N and 1.52 Å for O). Through a similar analysis, one can infer that all extended

TABLE 2: Comparison between Crystal and Calculated Structures for Systems A∼D

			basis functions[a]		rmsd[b]	
oligomer	number of atoms	helical type	whole system	largest subsystem	whole system	backbone only
A	77	single	885	460	0.38	0.38
B	106	single	1240	475	0.34	0.34
C	202	double	2330	550	0.78	0.70
D	490	double	5490	515	1.09	0.51

[a] With the 6-31G** basis set [b] The side chain refers to the BnO−CONH− groups at both two ends of the strand.

TABLE 3: Mean Helical Pitch of Oligomers A−D

oligomers	helical turn	mean helical pitch (Å)[a]
A	1	3.47
B	1.5	3.36
C	3	3.01
D	4	2.79

[a] The helical pitch refers to the distance along the helix axis between two layers in the same strand in **A** and **B**, and between two layers in different strands in **C** and **D**.

TABLE 4: Energies[a] of Different Conformers of Oligomer A Calculated with the 6-311+G Basis Set**

oligomer **A**	vdW correction	B3LYP(vdW)-GEBF
$E_{helical}$	−0.60477	−2328.79843
$E_{extended-1}$	−0.57802	−2328.76729
$E_{extended-2}$	−0.58442	−2328.77602
$\Delta E_{helical-(extended-1)}$	−16.78	−19.54
$\Delta E_{helical-(extended-2)}$	−12.77	−14.06

[a] E is in au and ΔE is in kcal/mol.

structures formed by rotating one or more of the CO−aryl or NH−aryl bonds would be energetically unfavorable relative to the helical structure, because the intramolecular hydrogen bonding interactions are maximized in the helical structure, in addition to the favorable $\pi-\pi$ interaction. Thus, the helical structure is intrinsically stable relative to other extended structures.

It is also interesting to know the contribution of the $\pi-\pi$ interaction to the formation of the helical structure from the extended structure. Again, we take the extended-2 structure as a reference structure. Among the energy difference between the helical and extended-2 structures ($E_{\text{helical}} - E_{\text{extended-2}} = -14.1$ kcal/mol), the vdW interaction contributes about −12.8 kcal/mol. So the contribution from the vdW interaction accounts for 91% of the total stabilization energy. This result reveals that the stacking interaction between neighboring pyridine rings plays a dominant role in maintaining the single-helical structure of **A**, and the intramolecular hydrogen bonds along the strand further stabilize the helical structure.

3.3. The Interstrand Interaction in the Formation of Double Helical Structures for Oligomers C and D. With the crystal structures of **C** and **D** as the initial structures, our B3LYP(vdW)-GEBF/6-31G** geometry optimizations also lead to two well-defined double-helical structures for these two molecules, as shown in Table 2 and Figure 3. The rmsd between the crystal and optimized structures is about 0.78 and 1.09 for **C** and **D**, respectively. If only the backbone atoms are considered, the rmsds are reduced to 0.70 and 0.51, respectively, for **C** and **D**. This result can be understood because the side-chain groups (especially in **D**) are very flexible (thus it is very difficult for our geometry optimizations to locate the global minimum structure). Nevertheless, the small rmsd values between the backbone atoms of the crystal and calculated structures for both compounds demonstrate the reliability of the B3LYP(vdW)-GEBF approach in predicting the geometries of complex supramolecules.

Next, we will investigate the driving forces for these two double-helical foldamers (**C** and **D**) to form the double-helical structures from the corresponding single-helical structures. Since the building blocks for **C** and **D** are very similar to those in **A** and **B**, the oligomers of **C** and **D** may easily form the corresponding single-helical structures. This result is borne out by our B3LYP(vdW)-GEBF geometry optimizations. Obviously, the dimerization energy ($E_{double} - 2E_{single}$) is an quantity to measure the driving force for the formation of a double-helical structure from two single-helical strands. For these two double-helical foldamers, the calculated dimerization energies are collected in Tables 5 and 6.

The calculated dimerization energy for **C** (with two pentameric strands) is about −44.7 kcal/mol (without the BSSE correction). For the dimer **C**, the BSSE correction (with 6-31G** basis set) calculated with the B3LYP(vdW)-GEBF approach is 0.07291 au, which is very close to the value (0.07351 au) obtained with conventional B3LYP(vdW) calculations. This result indicates that the GEBF approach is capable of providing accurate evaluation of the BSSE correction. After 50% BSSE correction is included, the dimerization energy reduces to −21.8 kcal/mol. Without the vdW corrections, we also optimize the structure of **C** with the B3LYP-GEBF/6-31G** approach, which leads to a significantly less compact structure (Figure S2). The calculated dimerization energy at this geometry turns out to be 2.89 kcal/mol (without BSSE correction), indicating that the interaction between two single strands is repulsive. This result provides clear evidence that the interstrand dispersion energy is responsible for the formation of **C**. For the dimer **D**, the dimerization energy between two nonameric strands (with vdW corrections and BSSE correction) is −22.6 kcal/mol. This result shows that the transformation from two single strands to a double-helix structure is an energetically favorable process for **C** and **D**, and the vdW energy between two single strands plays a dominant role in stabilizing the double-helical structure.

To investigate the dependence of the stability of the dimers on the strand length, we also calculate the dimerization energies for two longer homologues of **C**, **C′** (nonamer) and **C″** (tridecamer). The optimized geometrical parameters of the corresponding single- and double-helical structures are provided in the Supporting Information. After 50% BSSE correction is included, the dimerization energy is calculated to be −5.1 and 8.8 kcal/mol, respectively, for the constructed species **C′** and **C″**. This result shows that the driving force to form the double-helix dimer decreases significantly with increasing the strand length. For the longest homologue **C″**, the transformation from two single strands to the double-helix structure turns out to be energetically unfavorable. To further understand energy changes during the dimerization process, one may assume that the dimerization process occurs by two steps. First, a single strand needs to extend like a spring, then two "extended" strands interact through extensive $\pi-\pi$ overlaps to form a double-helical

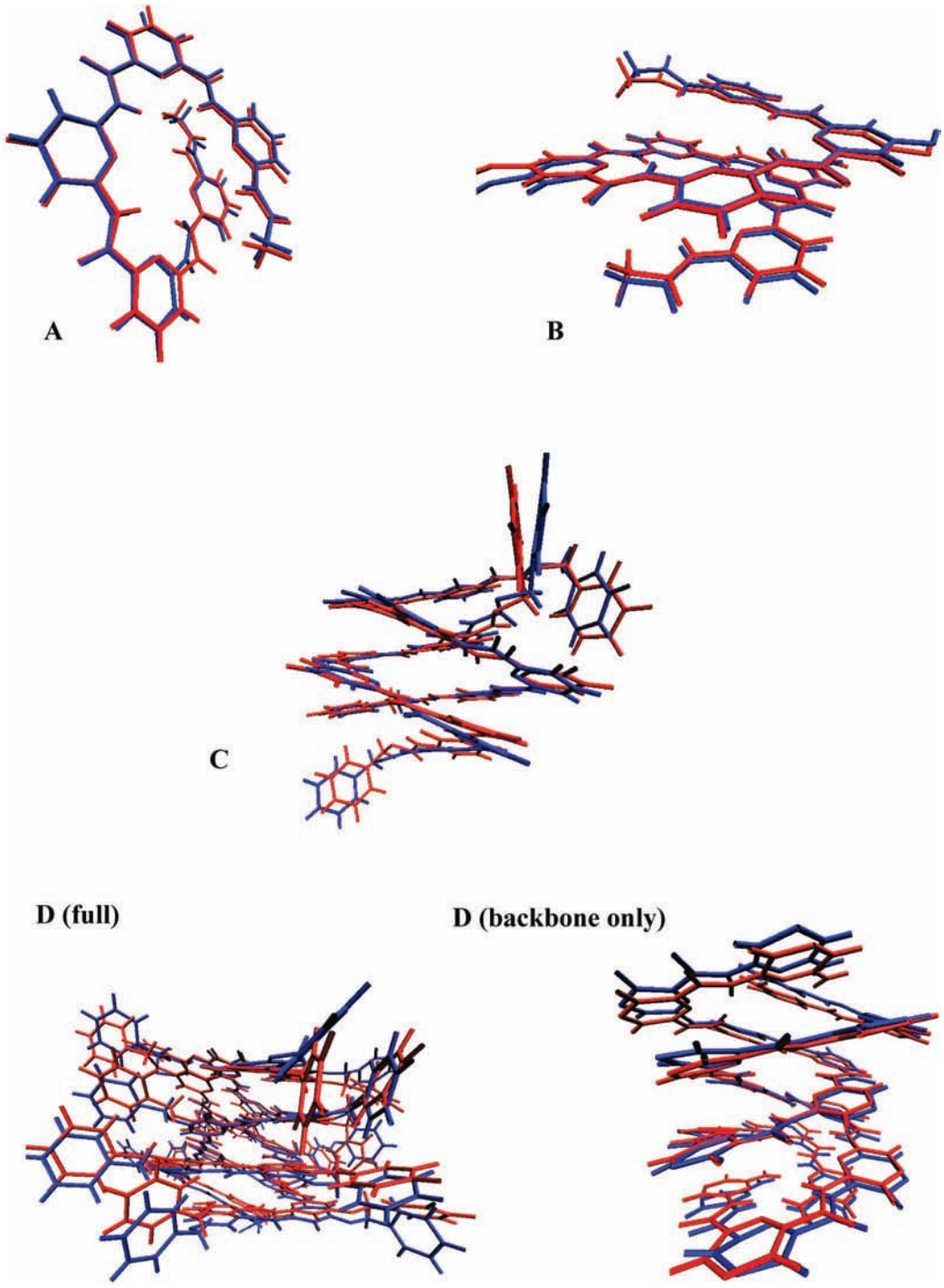

Figure 3. Superposition between the crystal structure (blue) and optimized structure (red) for oligomers **A**∼**D**.

TABLE 5: Energies[a] for Single Strands and the Double-Helical Dimer of Oligomer C Calculated with the 6-311+G Basis Set**

oligomer **C**	B3LYP(vdW)-GEBF	vdW correction	B3LYP-GEBF
$E_{monomer}$[b]	−3092.08260	−0.81608	−3091.29472
E_{dimer}	−6184.24199	−1.73773	−6182.58484
$E_{dimer} - 2E_{monomer}$	−48.19	−66.25	2.89

[a] E is in au; ΔE is in kcal/mol. [b] The geometry of the helical monomer is freely optimized.

structure.[92,93] The first step can be characterized by the "extension" energy, which is the energy cost from the freely optimized single-helical monomer to the corresponding monomer with the geometry in the dimmer, and the second step can be described with an quantity called as the vertical dimerization energy (VDE). Clearly, the (adiabatic) dimerization energy described above is the sum of the "extension" energy and the vertical dimerization energy (between two "extended" strands). Since two single strands in the dimers have different energies, the average value between the "extension" energies of two single strands is adopted here. For species **C**, **C**′, **C**″, and **D**, the calculated "extension" energy for each oligomeric strand is about 25.5 (**C**), 52.0 (**C**′), 84.2 (**C**″) and 86.9 kcal/mol (**D**), and the corresponding vertical dimerization energy between two "extended" strands is −72.7 (**C**), −109.1 (**C**′), −159.6 (**C**″), and

TABLE 6: Extension and Dimerization Energies (Calculated with the 6-311+G basis set) for Two Single-Helical Strands to Form Double-Helical Dimers in Four Oligomers: C, C′, C″, and D**

B3LYP(vdW)-GEBF	**C** (pentamer)	**C′** (nonamer)	**C″** (tridecamer)	**D** (nonamer)
$E_{monomer}$ (au)[a] strand-A	−3092.04785	−4756.12475	−6420.19902	−6799.27264
strand-B	−3092.04183	−4756.12093	−6420.19604	−6799.27224
$E_{monomer}$ (au)[b]	−3092.08542	−4756.20569	−6420.33171	−6799.41094
E_{dimer} (au)	−6184.24199	−9512.47838	−12840.73176	−13598.94762
50%BSSE (au)	0.03646	0.05886	0.08241	0.08968
$\Delta E_{extension}$ (kcal/mol)	25.46	51.99	84.20	86.91
$\Delta E_{VDE}^{50\%BSSE}$ (kcal/mol)	−72.70	−109.09	−159.57	−196.45
$\Delta E^{50\%BSSE}$ (kcal/mol)[c]	−21.77	−5.11	8.83	−22.63

[a] The monomer is at the geometry as shown in the dimer. [b] The geometry of the helical monomer is freely optimized. [c] The interaction energies without BSSE corrections are −44.65, −42.04 and −42.88 kcal/mol for **C**, **C′**, and **C″**, respectively.

−196.5 kcal/mol (**D**). From the calculated "extension" energies, one can see that for species **C**, **C′**, **C″**, and **D** the magnitude of both the "extension" energy and the vertical dimerization energy increase roughly linearly with strand length. However, the energy gain due to intermolecular $\pi-\pi$ stacking is larger than the sum of the "extension" energies needed by two single strands in species **C**, **C′**, and **D,** but is slightly less than that in **C″**. This result is in accord with the experimental facts that the formation of double-helical dimers with longer oligomeric strands is difficult.

As shown in previous experimental works,[25] dimerization constants of single helices of AOA's to form double helices increases with the strand length to reach a maximum and then decreases gradually down for longer oligomers. Since many factors (such as the entropic factor and the solvent effect) are not considered in the present work, we could not give clear-cut explanations for the experimental facts described above. The main conclusion from the present calculations is that the stability of the double-helical dimer (relative to two single strands) decreases with increasing the strand length, because the cost of the extension for two single strands can not be compensated by the energy gain from intermolecular $\pi-\pi$ stacking upon dimerization as the strands become longer.

4. Conclusions

In the present work, we have implemented the GEBF approach within the framework of the vdW-corrected DFT to investigate the energies and structures of several large supramolecular systems, in which the aromatic stacking interactions play a very important role. The optimized structures from B3LYP(vdW)-GEBF calculations are in good agreement with the corresponding crystal structures, verifying the reliability of the B3LYP(vdW)-GEBF approach. For two single-helical molecular strands (**A** and **B**) and two double-helical dimers (**C** and **D**) based on aromatic oligoamides, we have applied B3LYP(vdW)-GEBF calculations to elucidate the role of intra- and intermolecular interactions in the formation of single- and double-helical structures. Two main conclusions can be drawn: (1) the formation of the single helical structure is driven by the stacking interaction between neighboring aromatic rings, and further stabilized by the intramolecular hydrogen bonds along the backbone; (2) the dimerization of two single-helical strands to form a double-helical foldamer in **C** and **D** is an energetically favorable process, and the main driving force comes from the intermolecular (or interstrand) aromatic stacking. However, the dimerization energy decreases significantly for longer oligomeric strands, because the cost of the extension for two single strands could not be compensated by the energy gain from intermolecular $\pi-\pi$ stacking upon dimerization. We hope that the results from this study are helpful for experimentalists to better control various factors in synthesizing stable foldamers with other building blocks.

Acknowledgment. This work was supported by the National Natural Science Foundation of China (Grant Nos. 20625309 and 20833003), the National Basic Research Program (Grant No. 2004CB719901), and the Chinese Ministry of Education (Grant No. NCET-04-0450).

Supporting Information Available: Figures showing fragmentation schemes and optimized structures of oligomer **C** and tables of Cartesian coordinates of the systems under study. This material is available free of charge via the Internet at http://pubs.acs.org.

References and Notes

(1) Lamm, M. S.; Rajagopal, K.; Schneider, J. P.; Pochan, D. J. *J. Am. Chem. Soc.* **2005**, *127*, 16692.
(2) Matsuura, K.; Murasato, K.; Kimizuka, N. *J. Am. Chem. Soc.* **2005**, *127*, 10148.
(3) Koga, T.; Matsuoka, M.; Higashi, N. *J. Am. Chem. Soc.* **2005**, *127*, 17596.
(4) Zastavker, Y. V.; Asherie, N.; Lomakin, A.; Pande, J.; Donovan, J. M.; Schnur, J. M.; Benedek, G. B. *Proc. Natl. Acad. Sci U.S.A.* **1999**, *96*, 7883.
(5) Dobrzynska, D.; Jerzykiewicz, L. B. *J. Am. Chem. Soc.* **2004**, *126*, 11118.
(6) Tellini, V. H. S.; Jover, A.; Meijide, F.; Tato, J. V.; Galantini, L.; Pavel, N. V. *Adv. Mater.* **2007**, *19*, 1752.
(7) Schappacher, M.; Deffieux, A. *Science* **2008**, *319*, 1512.
(8) Lehn, J. M. *Proc. Natl. Acad. Sci USA* **2002**, *99*, 4763.
(9) Lehn, J. M. *Science* **2002**, *295*, 2400.
(10) Kato, T. *Science* **2002**, *295*, 2414.
(11) Fuhrhop, J.; Wang, T. Y. *Chem. Rev.* **2004**, *104*, 2901.
(12) Shimizu, T.; Masuda, M.; Minamikawa, H. *Chem. Rev.* **2005**, *105*, 1401.
(13) Hoeben, F. J. M.; Jonkheijm, P.; Meijer, E. W.; Schenning, A. P. H. J. *Chem. Rev.* **2005**, *105*, 1491.
(14) Berl, V.; Huc, I.; Khoury, R. G.; Krische, M. J.; Lehn, J. M. *Nature* **2000**, *407*, 720.
(15) Huang, B.; Parquette, J. R. *J. Am. Chem. Soc.* **2001**, *123*, 2689.
(16) Berl, V.; Huc, I.; Khoury, R. G.; Lehn, J. M. *Chem. Eur. J.* **2001**, *7*, 2798.
(17) Berl, V.; Huc, I.; Khoury, R. G.; Krische, M. J.; Lehn, J. M. *Chem. Eur. J.* **2001**, *7*, 2810.
(18) Huc, I.; Maurizot, V.; Gornitzka, H.; Léger, J. M. *Chem. Commun.* **2002**, 578.
(19) Jiang, H.; Léger, J. M.; Huc, I. *J. Am. Chem. Soc.* **2003**, *125*, 3448.
(20) Jiang, H.; Léger, J. M.; Dolain, C.; Guionneau, P.; Huc, I. *Tetrahedron* **2003**, *59*, 8365.
(21) Ernst, J. T.; Becerril, J.; Park, H. S.; Yin, H.; Hamilton, A. D. *Angew. Chem., Int. Ed.* **2003**, *42*, 535.
(22) Burkhart, B. M.; Langs, D. A.; Pangborn, W. A.; Duax, W. L.; Pletnev, V.; Gassman, R. M. *Biopolymers* **1999**, *51*, 129.
(23) Brunsveld, L.; Folmer, B, J. B.; Meijer, E, W.; Sijbesma, R. P. *Chem. Rev* **2001**, *101*, 4071.
(24) Hobza, P.; Šponer, J. *Chem. Rev.* **1999**, *99*, 3247.
(25) Jiang, H.; Maurizot, V.; Huc, I. *Tetrahedron* **2004**, *60*, 10029.
(26) Acocella, A.; Venturini, A.; Zerbetto, F. J. *J. Am. Chem. Soc.* **2004**, *126*, 2362.

(27) Lee, E. C.; Kim, D.; Jurecka, P.; Tarakeshwar, P.; Hobza, P.; Kim, K. S. *J. Phys. Chem. A* **2007**, *111*, 3446.
(28) Sinnokrot, M. O.; Sherrill, C. D. *J. Phys. Chem. A* **2006**, *110*, 10656.
(29) Schweizer, W. B.; Dunitz, J. D. *J. Chem. Theory Comput.* **2006**, *2*, 288.
(30) Hobza, P.; Ŝponer, J.; Polášek, M. *J. Am. Chem. Soc.* **1995**, *117*, 792.
(31) Sinnokrot, M. O.; Sherrill, C. D. *J. Phys. Chem. A* **2004**, *108*, 10200.
(32) Sinnokrot, M. O.; Sherrill, C. D. *J. Am. Chem. Soc.* **2004**, *126*, 7690.
(33) Arnstein, S. A.; Sherrill, C. D. *Phys. Chem. Chem. Phys.* **2008**, *10*, 2646.
(34) Ringer, A. L.; Sherrill, C. D. *Chem. Eur. J.* **2008**, *14*, 2542.
(35) (a) Bludsky, O.; Ŝponer, J.; Leszczynski, J.; Spirko, V.; Hobza, P. *J. Chem. Phys.* **1996**, *105*, 11042.
(36) Muller-Dethlefs, K.; Hobza, P. *Chem. Rew.* **2000**, *100*, 143.
(37) Ŝponer, J. *J. Am. Chem. Soc.* **2002**, *124*, 11802.
(38) Reha, D.; Kabeláč, M.; Ryjacek, F.; Ŝponer, J.; Ŝponer, J. E.; Elstner, M.; Suhai, S.; Hobza, P. *J. Am. Chem. Soc.* **2002**, *124*, 3366.
(39) Jurecka, P.; Hobza, P. *J. Am. Chem. Soc.* **2003**, *125*, 15608.
(40) Èerný, J.; Hobza, P. *Phys. Chem. Chem. Phys.* **2005**, *7*, 1624.
(41) Vondrasek, J.; Bendova, L.; Klusak, V.; Hobza, P. *J. Am. Chem. Soc.* **2005**, *127*, 2615.
(42) Hobza, P. *Phys. Chem. Chem. Phys.* **2008**, *10*, 2581–2583.
(43) Ŝponer, J.; Riley, K. E.; Hobza, P. *Phys. Chem. Chem. Phys.* **2008**, *10*, 2595.
(44) Kim, K. S.; Tarakeshwarm, P.; Lee, J. Y. *Chem. Rev.* **2000**, *100*, 4145.
(45) Hong, B. H.; Lee, J. Y.; Lee, C. W.; Kim, J. C.; Bae, S. C.; Kim, K. S. *J. Am. Chem. Soc.* **2001**, *123*, 10748.
(46) Tarakeshwar, P.; Choi, H. S.; Kim, K. S. *J. Am. Chem. Soc.* **2001**, *123*, 3323.
(47) Wu, Q.; Yang, W. T. *J. Chem. Phys.* **2002**, *116*, 515.
(48) Wu, X.; Vargas, M. C.; Nayak, S.; Lotrich, V.; Svoles, G. *J. Chem. Phys.* **2001**, *115*, 8748.
(49) Zimmerli, U.; Parrinello, M.; Koumoutsakos, P. *J. Chem. Phys.* **2004**, *120*, 2693.
(50) Grimme, S. *J. Comput. Chem.* **2004**, *25*, 1463.
(51) Grimme, S. *J. Comput. Chem.* **2006**, *27*, 1787.
(52) Antony, J.; Grimme, S. *Phys. Chem. Chem. Phys.* **2006**, *8*, 5287.
(53) Schwabe, T.; Grimme, S. *Phys. Chem. Chem. Phys.* **2006**, *8*, 4398.
(54) Schwabe, T.; Grimme, S. *Phys. Chem. Chem. Phys.* **2006**, *9*, 3397.
(55) Grimme, S. *Angew. Chem., Int. Ed.* **2008**, *47*, 3430.
(56) Jurecka, P.; Èerný, J.; Hobza, P.; Salahub, D. R. *J. Comput. Chem.* **2007**, *28*, 555.
(57) Mooij, W. T. M.; van Duijneveldt, F. B.; van Duijneveldt-van de Rijdt, J. G. C. M.; van Eijck, B. P. *J. Phys. Chem. A* **1999**, *103*, 9872.
(58) Li, S. H.; Li, W.; Fang, T. *J. Am. Chem. Soc.* **2005**, *127*, 7215.
(59) Yang, W. T. *Phys. Rev. Lett.* **1991**, *66*, 1438.
(60) Yang, W. T.; Lee, T.-S. *J. Chem. Phys.* **1995**, *103*, 5674.
(61) Li, S. H.; Ma, J.; Jiang, Y. S. *J. Comput. Chem.* **2002**, *23*, 237.
(62) Li, S. H.; Shen, J.; Li, W.; Jiang, Y. S. *J. Chem. Phys.* **2006**, *125*, 074109.
(63) Exner, T. E.; Mezey, P. G. *J. Phys. Chem. A* **2004**, *108*, 4301.
(64) Gu, F. L.; Aoki, Y.; Korchowiec, J.; Imamura, A.; Kirtman, B. *J. Chem. Phys.* **2004**, *121*, 10385.
(65) He, X.; Zhang, J. Z. H. *J. Chem. Phys.* **2005**, *122*, 031103.
(66) Chen, X.; Zhang, Y.; Zhang, J. Z. H. *J. Chem. Phys.* **2005**, *122*, 184105.
(67) Li, W.; Li, S. H. *J. Chem. Phys.* **2005**, *122*, 194109.
(68) Kobayashi, M.; Akama, T.; Nakai, H. *J. Chem. Phys.* **2006**, *125*, 204106.
(69) Akama, T.; Kobayashi, M.; Nakai, H. *J. Comput. Chem.* **2007**, *28*, 2003.
(70) Kobayashi, M.; Imamura, Y.; Nakai, H. *J. Chem. Phys.* **2007**, *127*, 074103.
(71) Fedorov, D. G.; Kitaura, K. *J. Chem. Phys.* **2004**, *120*, 6832.
(72) Fedorov, D. G.; Kitaura, K. *J. Chem. Phys.* **2005**, *122*, 134103.
(73) Fedorov, D. G.; Kitaura, K. *J. Phys. Chem. A* **2007**, *111*, 6904.
(74) Hirata, S.; Valiev, M.; Dupuis, M.; Xantheas, S. S.; Sugiki, S.; Sekino, H. *Mol. Phys.* **2005**, *103*, 2255.
(75) Sakai, S.; Morita, S. *J. Phys. Chem. A* **2005**, *109*, 8424.
(76) Li, W.; Li, S. *J. Chem. Phys.* **2004**, *121*, 6649.
(77) Deev, V.; Collins, M. A. *J. Chem. Phys.* **2005**, *122*, 154102.
(78) Collins, M. A.; Deev, V. A. *J. Chem. Phys.* **2006**, *125*, 104104.
(79) Bettens, R. P. A.; Lee, A. M. *J. Phys. Chem. A* **2006**, *110*, 8777.
(80) Jiang, N.; Ma, J.; Jiang, Y. *J. Chem. Phys.* **2006**, *124*, 114112.
(81) Li, W.; Fang, T.; Li, S. H. *J. Chem. Phys.* **2006**, *124*, 154102.
(82) Ganesh, V.; Dongare, R. K.; Balanarayan, P.; Gadre, S. R. *J. Chem. Phys.* **2006**, *125*, 104109.
(83) Li, W.; Li, S. H.; Jiang, Y. S. *J. Phys. Chem. A* **2007**, *111*, 2193.
(84) Li, S. H.; Li, W. *Annu. Rep. Prog. Chem., Sect. C: Phys. Chem.* **2008**, *104*, 256.
(85) Li, W.; Dong, H.; Li, S. H. *Progress in Theoretical Chemistry and Physics*; Springer-Verlag: Berlin and Heidelberg, Germany, 2008; Vol. 18, p 289.
(86) Boys, S. F.; Bernardi, F. *Mol. Phys.* **1970**, *19*, 553.
(87) Frisch, M. J.; Trucks, G. W.; Schlegel, H. B.; Scuseria, G. E.; Robb, M. A.; Cheeseman, J. R. ; Montgomery J. A., Jr.; Vreven, T.; Kudin, K. N.; Burant, J. C.; Millam, J. M.; Iyengar, S. S.; Tomasi, J.; Barone, V.; Mennucci, B.; Cossi, M.; Scalmani, G.; Rega, N.; Petersson, G. A.; Nakatsuji, H.; Hada, M.; Ehara, M.; Toyota, K.; Fukuda, R.; Hasegawa, J.; Ishida, M.; Nakajima, T.; Honda, Y.; Kitao, O.; Nakai, H.; Klene, M.; Li, X.; Knox, J. E.; Hratchian, H. P.; Cross, J. B.; Bakken, V.; Adamo, C.; Jaramillo, J.; Gomperts, R.; Stratmann, R. E.; Yazyev, O.; Austin, A. J.; Cammi, R.; Pomelli, C.; Ochterski, J. W.; Ayala, P. Y.; Morokuma, K.; Voth, G. A.; Salvador, P.; Dannenberg, J. J.; Zakrzewski, V. G.; Dapprich, S.; Daniels, A. D.; Strain, M. C.; Farkas, O.; Malick, D. K.; Rabuck, A. D.; Raghavachari, K.; Foresman, J. B.; Ortiz, J. V.; Cui, Q.; Baboul, A. G.; Clifford, S.; Cioslowski, J.; Stefanov, B. B.; Liu, G.; Liashenko, A.; Piskorz, P.; Komaromi, I.; Martin, R. L.; Fox, D. J.; Keith, T.; Al.Laham, M. A.; Peng, C. Y.; Nanayakkara, A.; Challacombe, M.; Gill, P. M. W.; Johnson, B.; Chen, W.; Wong, M. W.; Gonzalez, C.; Pople, J. A. Gaussian, Inc.: Wallingford CT, 2004.
(88) Dolain, C.; Zhan, C. L.; Léger, J. M.; Daniels, L.; Huc, I. *J. Am. Chem. Soc.* **2005**, *127*, 2400.
(89) Haldar, D.; Jiang, H.; Léger, J. M.; Huc, I. *Angew. Chem., Int. Ed.* **2006**, *45*, 5483.
(90) Humphrey, W.; Dalke, A.; Schulten, K. *J. Mol. Graphics* **1996**, *14*, 33.
(91) Èerný, J.; Kabeláč, M.; Hobza, P. *J. Am. Chem. Soc.* **2008**, *130*, 16055.
(92) Huc, I. *Eur. J. Inorg. Chem.* **2004**, 17.
(93) Haldar, D.; Jiang, H.; Léger, J. M.; Huc, I. *Tetrahedron* **2007**, *63*, 6322.

JP8071525